

## Magnetization reversal processes in epitaxial Fe/GaAs(001) films

C. Daboo, R. J. Hicken, D. E. P. Eley, M. Gester, S. J. Gray et al.

Citation: *J. Appl. Phys.* **75**, 5586 (1994); doi: 10.1063/1.355649

View online: <http://dx.doi.org/10.1063/1.355649>

View Table of Contents: <http://jap.aip.org/resource/1/JAPIAU/v75/i10>

Published by the [American Institute of Physics](http://www.aip.org).

---

### Related Articles

In situ control of electronic phase separation in La<sub>1/8</sub>Pr<sub>4/8</sub>Ca<sub>3/8</sub>MnO<sub>3</sub>/PNM-PT thin films using ferroelectric-poling-induced strain

*J. Appl. Phys.* **113**, 013705 (2013)

Transport and magnetic properties of Fe doped CaMnO<sub>3</sub>

*J. Appl. Phys.* **112**, 123913 (2012)

Simulations of magnetic nanoparticle Brownian motion

*J. Appl. Phys.* **112**, 124311 (2012)

Ferromagnetism, hysteresis and enhanced heat dissipation in assemblies of superparamagnetic nanoparticles

*J. Appl. Phys.* **112**, 114912 (2012)

Defect mediated reversible ferromagnetism in Co and Mn doped zinc oxide epitaxial films

*J. Appl. Phys.* **112**, 113917 (2012)

---

### Additional information on *J. Appl. Phys.*

Journal Homepage: <http://jap.aip.org/>

Journal Information: [http://jap.aip.org/about/about\\_the\\_journal](http://jap.aip.org/about/about_the_journal)

Top downloads: [http://jap.aip.org/features/most\\_downloaded](http://jap.aip.org/features/most_downloaded)

Information for Authors: <http://jap.aip.org/authors>

## ADVERTISEMENT



**AIP Advances**

Now Indexed in Thomson Reuters Databases

Explore AIP's open access journal:

- Rapid publication
- Article-level metrics
- Post-publication rating and commenting

# Magnetization reversal processes in epitaxial Fe/GaAs(001) films

C. Daboo, R. J. Hicken, D. E. P. Eley, M. Gester, S. J. Gray, A. J. R. Ives, and J. A. C. Bland

*Cavendish Laboratory, University of Cambridge, Madingley Road, Cambridge CB3 0HE, United Kingdom*

In this article we present the results of a detailed study of the switching behavior observed in epitaxial single Fe films of thickness between 30 and 450 Å, and a wedge shaped Fe film with a thickness range of 10–60 Å grown on GaAs (001). These films have cubic and uniaxial anisotropies which change with film thickness. For the fixed thickness films the values of the anisotropy constants were accurately determined by Brillouin light scattering (BLS) measurements together with polar magneto-optic Kerr effect (MOKE) measurements that gave the value of the magnetization. The switching behavior of these samples was observed with in-plane MOKE magnetometry as a function of the angle between the applied field and the in-plane crystallographic axes. Measurements of the component of magnetization perpendicular to the applied field allow a precise determination of the relative orientation of the hard and easy in-plane anisotropy axes. This can be used to accurately determine the ratio of uniaxial to cubic anisotropy constants, when this ratio is less than one. The ratios obtained from MOKE agree well with those obtained from BLS. Minimum energy calculations predict that the reversal process should proceed by a continuous rotation of the magnetization vector with either one or two irreversible jumps, depending on the applied field orientation and the nature of the anisotropy of the film. The calculations provide a good qualitative description of the observed reversal process, although the magnetic microstructure influences the exact values of the switching fields.

## I. INTRODUCTION

A number of groups have reported magneto-optic Kerr effect (MOKE)  $M$ - $H$  loops for the component of magnetization parallel to the applied field ( $M_{\parallel}$ ) which show “overshoots” which depend on the analyzer setting chosen to observe the MOKE signal.<sup>1</sup> This has been explained as an additional optical effect caused by “mixing in” a contribution caused by the component of magnetization perpendicular to the applied field ( $M_{\perp}$ ).<sup>1</sup> It is the different magnetic switching behavior observed in  $M_{\parallel}$  and  $M_{\perp}$  that produces the overshoots in the  $M_{\parallel}$ - $H$  MOKE loops.<sup>2,3</sup> Here we extend the previous studies of this system<sup>2-4</sup> to show how the detailed switching behavior is expected to vary with precise orientation of the applied field and the exact ratio  $r$  of uniaxial to cubic anisotropy constants ( $r = K_u/K_1$ ), which are known to be present in such samples.<sup>4</sup>

## II. EXPERIMENTAL PROCEDURES

The samples were grown under ultrahigh vacuum (UHV) conditions (pressure during evaporation less than  $\sim 5 \times 10^{-10}$  mbar) on GaAs (001) substrates and studied by low-energy electron diffraction LEED, Auger spectroscopy, and *in situ* MOKE. The substrates were held at 150 °C during Fe growth at  $\sim 1 \text{ \AA min}^{-1}$  from the  $e$ -beam evaporator. A series of samples with thickness between 30 and 450 Å were grown, together with a wedge shaped Fe film in the thickness range of 10–60 Å. Each was capped with  $\sim 20 \text{ \AA}$  of Cr. The *in situ* MOKE was used to study the evolution of the magnetic anisotropy as the Fe films were grown<sup>5</sup> so that films with different final anisotropy strengths could be produced.

The fixed thickness samples were characterized *ex situ* using Brillouin light scattering (BLS) and polar MOKE to determine the anisotropy constants  $K_1$  and  $K_u$  of each sample. By fitting the BLS data as a function of the angle  $\phi$

between the applied field direction and the hard uniaxial anisotropy axis it was possible to determine the quantities  $2K_1/M$  and  $2K_u/M$ . The saturation field determined from the polar MOKE gave the value of the magnetization  $M$  in the samples, ignoring any surface anisotropy, thus allowing the anisotropy constants to be determined from the combined measurements. The thickness dependence of the anisotropy is reported elsewhere,<sup>5</sup> but in general it was found that thinner Fe layers had a larger anisotropy ratio  $r$ , and a reduced average magnetization. Due to the uniaxial anisotropy which was found to be parallel to a  $\langle 110 \rangle$  direction, the two  $\langle 110 \rangle$  directions in the sample are inequivalent as one is a hard cubic axis and hard uniaxial axis (the hard-hard axis) while the other is a hard cubic axis and easy uniaxial axis (the hard-easy axis).

For the MOKE measurements the sample and an electromagnet were separately mounted on two concentric precision ( $0.001^\circ$  step) rotary stepper drives, so that they could each be turned independently to any desired orientation over the full  $0^\circ$ – $360^\circ$  range under computer control. The MOKE technique used here measures MOKE  $M$ - $H$  loops for two orientations of the applied field, namely, parallel and perpendicular to the plane of incidence of the light. By using the same optical geometry for each measurement it was possible to determine  $M_{\parallel}$  and  $M_{\perp}$  directly from the resulting loops.<sup>6,7</sup>

## III. RESULTS

In general it was found that the magnitude of the magnetization vector remained virtually constant during the reversal process indicating that the sample behaved as a single domain, except very close to a switching field value. Figure 1 shows three typical sets of MOKE loops illustrating the different switching behavior observed in our samples. These loops were taken from the wedge shaped Fe film for an an-

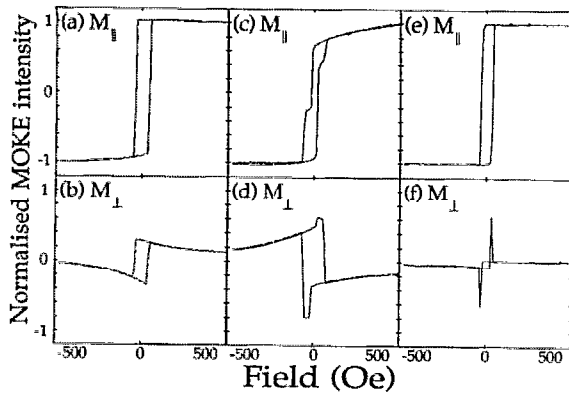


FIG. 1. Typical MOKE loops for the Fe wedged film for  $r=0.4\pm 0.02$ . (a)  $M_{\parallel}$ - $H$  and (b)  $M_{\perp}$ - $H$  loops at  $\phi=75^{\circ}$ . (c)  $M_{\parallel}$ - $H$  and (d)  $M_{\perp}$ - $H$  loops at  $\phi=20^{\circ}$ . (e)  $M_{\parallel}$ - $H$  and (f)  $M_{\perp}$ - $H$  loops at  $\phi=60^{\circ}$ .

isotropy ratio  $r=0.4\pm 0.02$ . Figures 1(a) and 1(b) show  $M_{\parallel}$ - $H$  and  $M_{\perp}$ - $H$  loops, respectively, for  $\phi=75^{\circ}$ . Both loops show one irreversible jump at the same field of  $\sim 50$  Oe as the field is reversed, corresponding to "one-jump" switching. Figures 1(c) and 1(d) show  $M_{\parallel}$ - $H$  and  $M_{\perp}$ - $H$  loops, respectively, for  $\phi=20^{\circ}$ . Here both loops show two irreversible jumps as the field is reversed, corresponding to "two-jump" switching. These two jumps each occur when the magnetization traverses each of the two hard axis directions that exist in a sample with  $|r|<1$ . This implies that when the uniaxial anisotropy dominates over the cubic anisotropy (i.e.,  $|r|>1$ ) only one-jump switching should occur, and this behavior is indeed observed. Figures 1(e) and 1(f) show  $M_{\parallel}$ - $H$  and  $M_{\perp}$ - $H$  loops, respectively, for  $\phi=60^{\circ}$ . In this case a "reversed" two-jump switch occurs since the magnetization initially rotates away from the field direction in a clockwise sense, say, but switches back over the field direction in an anticlockwise sense.

In order to study the magnetic switching behavior in more detail we used a coherent rotation model<sup>8</sup> to calculate the shape of the  $M_{\parallel}$ - $H$  and  $M_{\perp}$ - $H$  loops, for various values of  $\phi$  and  $r$ . These calculations indicated that the reversal process can proceed either by one or two jumps depending on the exact values of  $\phi$  and  $r$ . It is possible to understand the calculated switching behavior by tracking local energy minima as a function of applied field strength. The reversal process starts off with the magnetization sitting in the positive saturation energy minimum with an orientation close to the applied field direction. As the field reverses this minimum becomes shallower and eventually disappears. At this point the magnetization undergoes an irreversible jump and falls into a different energy minimum. In the one-jump switching process this second minimum is the negative saturation energy minimum, and the magnetization remains in this minimum as the applied field is taken towards negative saturation. In the two-jump switching process, there is a third intermediate energy minimum that exists when the positive saturation minimum disappears, with the result that the magnetization falls into this minimum in preference to the negative saturation minimum. However, as the field is further reversed this intermediate minimum also disappears and the

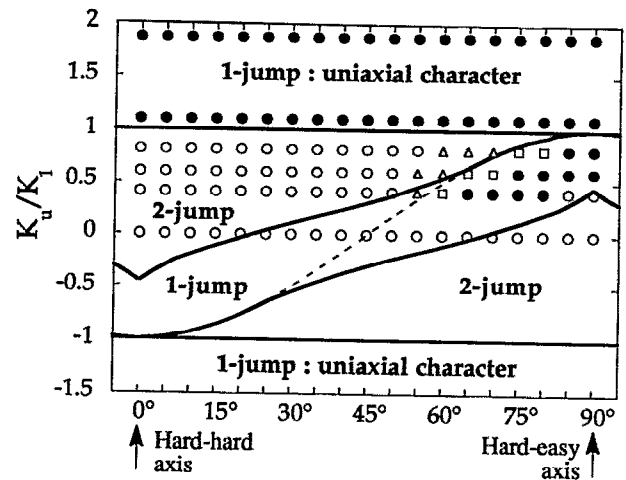


FIG. 2. Calculated and experimental phase diagram of one- and two-jump switching as a function of applied field orientation  $\phi$  and anisotropy ratio  $r$ . The solid lines indicate the calculated boundary between one- and two-jump switching, while the dashed line shows the calculated position of the easy axis. Experimental switching is indicated by the symbols:  $\bullet$ —one-jump switching;  $\circ$ —normal two-jump switching;  $\square$ —reverse two-jump switching;  $\triangle$ —cannot discriminate between one- or two-jump switching.

magnetization eventually ends up in the negative saturation energy minimum. For one-jump switching it is also possible that the intermediate minimum is initially present, but disappears just before the positive saturation minimum disappears. However, in real magnetic films the magnetization can switch via domain wall sweeping *before* the positive saturation minimum has disappeared, and *before* the intermediate minimum has disappeared with the result that a two-jump switch occurs when the calculations predict a one-jump switch, and in this case two possibilities occur. When  $\phi$  is on the hard-hard axis side of the easy axis, normal two-jump switching is seen to occur [Figs. 1(c) and 1(d)]. When  $\phi$  is on the hard-easy axis side of the easy axis a reverse two-jump switch is seen [Figs. 1(e) and 1(f)].

The switching processes are illustrated in Fig. 2, which shows the calculated phase diagram for one- and two-jump switching as a function of  $\phi$  and  $r$ . The boundary between the one- and two-jump switching regimes is shown by a solid line, and is defined as the point at which the intermediate and positive saturation minima both disappear at the same applied field. A simple expression for the angle  $\theta$  between the hard-hard axis and the easy axis, shown by the dashed line on Fig. 2, is given by

$$\begin{aligned} \cos 2\theta &= -r, \quad \text{for } |r| \leq 1, \\ \theta &= 90^{\circ}, \quad \text{for } |r| \geq 1. \end{aligned} \quad (1)$$

Experimental results for three samples with anisotropy ratios of  $\sim 0$  (sample 1—almost completely cubic), 0.4, 0.6, 0.8, and 1.1 (sample 2—various positions along the wedge shaped sample), and 1.8 (sample 3—strongly uniaxial) are also shown at  $5^{\circ}$  intervals with different symbols to indicate different switching behavior. For  $|r|>1$  the calculations show that only one-jump switching can occur, and this is confirmed by the experimental results for sample 3 and sample 2 (with  $r=1.1$ ). The results for sample 2 (with

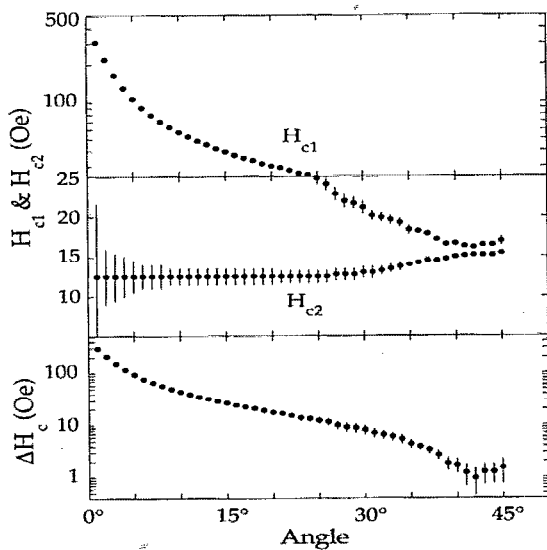


FIG. 3. The two-jump switching fields  $H_{c1}$  and  $H_{c2}$  (top panels), and their difference  $\Delta H_c$  (bottom panel) as a function of applied field orientation  $\phi$ .

$r=0.4, 0.6,$  and  $0.8$ ) are in good agreement with the calculations, though close to the easy axis it is difficult to discriminate between one- and two-jump switching. Reverse two-jump loops are only seen on the hard-easy axis side of the easy axis. For sample 1, the observed switching behavior conflicts with that predicted by the calculations since two-jump switching is always present indicating that domain wall sweeping can be more easily induced when  $r$  is close to zero.

For two-jump switching, as  $\phi$  approaches an easy axis the difference  $\Delta H_c$  between the two switching fields  $H_{c1}$ , defined as the larger switching field, and  $H_{c2}$  is reduced, and very close to the easy axis  $\Delta H_c$  can be  $\sim 2$  Oe. The dependence of  $H_{c1}$ ,  $H_{c2}$ , and  $\Delta H_c$  on  $\phi$  is shown in Fig. 3 for sample 1, as  $\phi$  varies between  $0^\circ$  (hard axis) and  $45^\circ$  (easy axis).  $H_{c2}$  is seen to remain almost constant at  $\sim 12$  Oe up to  $\phi \approx 30^\circ$ , beyond which it gradually increases to  $\sim 15$  Oe at  $\phi = 45^\circ$ . However,  $H_{c1}$  changes rapidly from  $\sim 300$  Oe down to  $\sim 25$  Oe at  $\phi \approx 30^\circ$ , and then gradually decreases to  $\sim 17$  Oe at  $\phi = 45^\circ$ . Thus  $\Delta H_c$  changes from  $\sim 300$  Oe at  $\phi = 0^\circ$  to  $\sim 2$  Oe at  $\phi = 45^\circ$ , providing a tuneable switching behavior that may be of use in device applications.

When the applied field direction is close to a hard or easy axis, the magnetization vector moves, respectively, away from or towards the axis as the field is reduced. Therefore, depending on which side of the anisotropy axis the field is applied, the magnetization will move either in a clockwise or anticlockwise sense. A change in the clockwise or anti-

clockwise motion of the magnetization can be clearly seen in  $M_\perp$ - $H$  MOKE loops, and by using high precision rotary stepper drives to turn the sample and align the magnet, it is possible to accurately determine the angles of the hard and easy axes in the sample plane. Since the angle between the easy axis and the hard-hard axis varies with  $r$ , as given by Eq. (1), it is possible to determine  $r$  when  $|r| < 1$  from MOKE measurements, and these values agree well with those determined by BLS. However, for the case of  $|r| \geq 1$  MOKE cannot be used to determine  $r$  directly.

#### IV. SUMMARY

We have studied the switching behavior of Fe/GaAs samples for various values of uniaxial and cubic anisotropy constants using in-plane MOKE magnetometry. Coherent rotation calculations showed that the switching mechanism depends on  $\phi$  and  $r$ . In general, the observed switching behavior agreed well with the switching mechanism predicted by the calculations, though in some cases domain wall sweeping caused two-jump switching where one-jump switching was expected from the calculation. The two-jump switching fields were found to depend on  $r$ , and for a field applied close to the cubic easy axis the difference in the switching fields could be as little as 2 Oe. It was found that  $r$  could be accurately found from the MOKE data by determining the angles at which the magnetization switched between a clockwise or anticlockwise motion. A simple analytical expression for this angle was given, and the experimental results for  $r$  determined from MOKE agreed well with that found from the BLS measurements. Since the sample behaves mostly as a single domain and the switching process is controllable, this behavior is of interest for device applications.

#### ACKNOWLEDGMENTS

The financial support of the SERC, the Toshiba Corporation, and the Newton Trust, Cambridge for this work is gratefully acknowledged. M. G. would like to thank the EC for a bursary (Contract No. BREU-900293). S. J. G. would like to thank the DRA, UK for support.

<sup>1</sup>J. M. Florczak and E. D. Dahlberg, J. Appl. Phys. **67**, 7520 (1990).

<sup>2</sup>J. M. Florczak and E. D. Dahlberg, Phys. Rev. B **44**, 9338 (1991).

<sup>3</sup>J. M. Florczak and E. D. Dahlberg, J. Magn. Magn. Mater. **104**, 399 (1992).

<sup>4</sup>J. J. Krebs, B. T. Jonker, and G. A. Prinz, J. Appl. Phys. **61**, 2596 (1987).

<sup>5</sup>C. Daboo *et al.* (to be published).

<sup>6</sup>C. Daboo, J. A. C. Bland, R. J. Hicken, A. J. R. Ives, M. J. Baird, and M. J. Walker, Phys. Rev. B **47**, 11852 (1993).

<sup>7</sup>C. Daboo, J. A. C. Bland, R. J. Hicken, A. J. R. Ives, M. J. Baird, and M. J. Walker, J. Appl. Phys. **73**, 6368 (1993).

<sup>8</sup>B. Dieny, J. P. Gavigan, and J. P. Rebouillat, J. Phys. C **2**, 159 (1990).